

# Effects of Tritonx100 and Tetraethylorthosilicate on the Morphology and Photocatalyst Properties of TiO<sub>2</sub> Thin Film

Hamideh Samari Jahromi<sup>1</sup>

<sup>1</sup> Research Institute of Petroleum Industry (RIPI), Environment Division, Tehran, Iran

E-mail: samarih@ripi.ir

Received: 10 Jul. 2013, Revised: 11 Jul. 2013; Accepted: 16 Aug. 2013

Published online: 1 Sep. 2013

**Abstract:** The effects of non-ionic Triton X-100 (TX) surfactant and Tetraethylorthosilicate binder agent for preparing the TiO<sub>2</sub> (TO) thin film were investigated. TO thin film was prepared using tetra chloride titanium as a precursor via an acid catalyzed sol-gel process. The morphology and surface structure of the films were studied by scanning electron microscopy (SEM) and atomic force microscopy (AFM). The structure and surface of films obtained by a dip-coating technique were found to depend strongly on the use and type of additive molecules added. The results show that, the film from titania sol without various additives molecules consists of agglomerated titania particles and ill-defined surface, which may cause the surface to be non-uniform, whereas Titania /TX-100 (TO-TX) sols resulted in the homogeneous and crack-free TO anatase films. Thin film deposited on SiO<sub>2</sub>-coated glass substrate indicate a packed and dense structure of the TO film. Many fine pores with different sizes existed in the TiO<sub>2</sub>-SiO<sub>2</sub> films (TO-SO). Dense structure with conformal coverage on SO is observed for TO film. A cross-sectional morphology of the thin films by one and six times of coating is investigated. It can be observed, grain size and thickness increase with increasing the number of coating times. It should be mentioned that film thickness for the one and six times of coating are 181nm and 205 nm respectively. Furthermore the photocatalytic decomposition of MCB for TO, TO-TX, TO-SO and TO-TX-SO thin films was measured as 13.2%, 53.72%, 86.02% and 97.45%, respectively. The results indicated that SO and TX had a significant effect on the morphology and photocatalytic properties of TO thin film.

**Keywords:** Thin film, Triton X100, Tetraethylorthosilicate, photocatalytic activity, Monochlorobenzene

## 1. Introduction

The photocatalytic properties of titanium oxide (TiO<sub>2</sub>) may result in a promising reactive technique for the removal of pollutants from air or water as self-cleaning surfaces and anti-algal coatings can be produced because of the biological and chemical stability, high photoactivity, low-toxicity and low cost of TiO<sub>2</sub> [1-2]. The ability of TiO<sub>2</sub> nanoparticles to destabilize cell membrane after in vitro exposure of cell lines has already been noted by some authors [3-5]. Nanosized TiO<sub>2</sub> is known to disrupt cell membrane stability as a result of its photocatalytic properties [6]. Destabilization of the cell membrane is undoubtedly among the primary effects of nano-TiO<sub>2</sub> and, therefore, suitable as a measure of the biological potential of such nanoparticles. Although the preparation of nano-TiO<sub>2</sub> is well established, one problem still generally exists during production: commercial TiO<sub>2</sub> usually consists of small particles while it is difficult and expensive to separate and recover these ultrafine particles from the suspension

after purification [7] especially when it coexists with multi-charged ions. For example, separation of the insoluble catalyst from the suspension is difficult because the suspended particles tend to aggregate especially at high concentration. In addition, application of suspended  $\text{TiO}_2$  (slurry) in purification system requires post-treatment for removal of the excessive turbidity of the treated samples, especially since there are recent concerns of  $\text{TiO}_2$  nanoparticle toxicity [8]. Filtration and precipitation are the most common post treatment processes for removal of the titania particles. The immobilization of the  $\text{TiO}_2$  in the form of a thin film not only provides an advantage over the drawbacks encountered with powder suspension, but could also endow the surface with photoinduced hydrophilicity [9]. Currently, the supporting technologies include preparing dense porous  $\text{TiO}_2$  films or coatings by different processes such as the sol-gel process [10], hydrothermal methods [11-13], reactive methods [14], sputtering [15], chemical vapor deposition [16] pulsed laser deposition [17] or fibers as a carrier medium. Among them, the relatively simple sol gel method is the most widely used technique due to the advantage of particles production in a relatively shorter processing time at lower temperatures [18]. In the sol gel process, there are different methods for sol deposition on the substrate such as spraying, electrophoresis, inject printing, dip coating and spin coating. Dip coating technique offers many advantages over other deposition techniques due to the use of very simple equipment. In addition, the stoichiometry and the high homogeneity of the final film can be controlled. In this method, the substrate to be coated is immersed in a liquid and then withdrawn at a well-defined speed under controlled temperature and atmospheric conditions [19]. However, controlling the synthesis and deposition is difficult, making it difficult to produce a thick crack free and homogeneous coating. In addition, the derived  $\text{TiO}_2$  films or coatings often have low reactive surface areas, low photocatalytic efficiency and high cost. A number of researchers have found ways to stabilize the anatase phase at high temperature and to optimize the photoactivity of titania by doping with different additives. Liu et al. also used the optimized  $\text{Ti}(\text{OC}_4\text{H}_9)_4\text{-P123-EtOH-HCl}$  system for the preparation of nano-crystalline  $\text{TiO}_2$  thin films [20]. Zhang et al. studied the effect of the molecular weight of ethylene glycol (PEG) and the molar ratio of the structure-directing agent in the sol-gel method [21], which is similar to our hydrothermally assisted sol-gel method by using P123 [22] and PEG [23] as templates. Cernigoj et al. utilized several commercially available, non-ionic surfactants (Brij 56, Pluronic F-127, and Triton X-100) with polyether chains of different lengths by applying them in the sol gel process with the titanium isopropoxide precursor to induce nanocrystallinity in the resulting inorganic films in an attempt to increase their photocatalytic activity for degradation of organic pollutants in waste water. In all the above cases, Ultra violet light and Visible light were used to activate  $\text{TiO}_2$  [24].

The mixed oxides  $\text{Al}_2\text{O}_3/\text{TiO}_2$ ,  $\text{ZrO}_2/\text{TiO}_2$ ,  $\text{SnO}_2/\text{TiO}_2$  and  $\text{SiO}_2/\text{TiO}_2$  with different dosage rates and various preparation methods have been investigated and reported [25-28]. The most common way to produce  $\text{SiO}_2/\text{TiO}_2$  materials is through a sol-gel process where the preparation of titania sol and silica sol is carried out separately and then they are mixed at various ratios to achieve the desired outcome [29-32] or they are prepared by direct formation. A second method is to introduce  $\text{TiO}_2$  into a presynthesized or commercial silica-containing material such as honeycomb ceramics [33], pillared clays [34], Y-zeolite [35], c-zeolite [36], MCM-41 [37], SiC [38], polymers [39] or ordered  $\text{SiO}_2$  materials in a post modification method. To obtain a high quality of  $\text{TiO}_2$  thin film used in photocatalysis processes for contaminant removal from air and water purification, it is necessary to investigate in detail the factors which may have important effects on the film properties [40]. Up to now, much work has been devoted to investigate the influence of different conditions on growth and structure of titania particles in the sols. For example it was found that complex agents (such as acetylacetone, diethanolamine and polyethylene

glycol) have different influences on the sols prepared in a sol gel dip coating process [41-45]. Other investigations have studied more factors such as the effect of calcination temperature which usually affects film structure [45-47] and adhesion strength between the films and the substrates [43, 46]. In this research, TiO<sub>2</sub> thin film was deposited on the glass substrates using a dip coating technique. The morphology and photocatalytic properties of the thin film were investigated by addition of non-ionic (Triton X-100) surfactant and Tetraethylorthosilicate binder agent. Since these parameters affect films morphology leading to variation of photocatalytic activity, decomposition of monochlorobenzene was selected as a model reaction in order to evaluate photocatalytic activity of the films.

## 2. Experimental details

### 2.1. Preparation of titania sol

For preparation of preliminary TiO<sub>2</sub> sol, the following materials were used: Tetra chloride titanium (TiCl<sub>4</sub>, M=189.79 gmol<sup>-1</sup>, 99%, Merck ), Nitric Acid (HNO<sub>3</sub>, M=63 gmol<sup>-1</sup>, 63%, Merck), Ammonia (NH<sub>3</sub>, M=17 gmol<sup>-1</sup>, 25%, Merck), polyoxyethylene isooctyl phenyl ether (Triton X-100, 99.5%, Merck), Ethanol (C<sub>2</sub>H<sub>5</sub>OH, M=46 gmol<sup>-1</sup>, 99.5%, Merck ), Triethanolamine (TEA, N(C<sub>2</sub>H<sub>5</sub>OH)<sub>3</sub>, M=149.10 gmol<sup>-1</sup>, 98%, Merck) and Tetraethylorthosilicate (TEOS, Si(OC<sub>2</sub>H<sub>5</sub>)<sub>4</sub>, M=208.33 gmol<sup>-1</sup>, 98%, Merck.) 1000 ml of deionized water was added to 2 ml TiCl<sub>4</sub> as starting material to form a suspension. Then, 45 ml of HNO<sub>3</sub> ([H<sup>+</sup>]/[Ti<sup>+</sup>]=0.5) was added to 500 ml of the suspension, including 12 mol of titanium and the suspension stirred for about 7 h. Subsequently, in order to produce a stable sol, this sol was placed in an 80 °C bath for 24 h. Therefore, a stable titanium oxide sol was formed. All of the above procedure for sol production was performed in the room temperature. The resulting sol is denoted as TO.

### 2.2. Preparation a mixture of acid titania and TX100

In order to prepare acid sol (pH=2), 10 ml preliminary titania sol described in the previous section was added to water (5 ml) and nitric acid (1 ml) , and they were stirred at room temperature for about 9 h while the sol was under reflux. The sol formed was dissolved in the mixture containing 35 ml of ethanol and 35 ml of water. Finally, three solutions of TO-TX were prepared separately by adding different amounts of triton X100 (1, 3 and 5 drops) as a surfactant. The resulting sol is denoted as TO-TX.

### 2.3. Preparation of Silica film

Silica sol was prepared from a 20ml tetraethylorthosilicate (TEOS, Aldrich) precursor, ethanol (Si/ EtOH = 0.15), HNO<sub>3</sub> (HNO<sub>3</sub>/ Si= 0.265) and water (H<sub>2</sub>O/Si= 8.1). After two hours of mixing, the resulting solution was used for silica film deposition by the dip-coating technique with pulling speeds up to 5 cm min<sup>-1</sup>. The resulting film is denoted as SO. The sol was unstable and therefore, was always freshly prepared. All silica films were produced by a single dipping. The silica films on soda-lime glass were used as substrates for the preparation of thin films that will be described in next section.

## 2.4. Thin film preparation and coating process

TO thin films were deposited at room temperature on soda lime glass by dip coating method (20ml of sol, dip- speed of 10 cm min<sup>-1</sup>). In the dip-coating method the substrate is slowly dipped into and withdrawn from a tank containing the sol, with a uniform velocity, in order to obtain a uniform coating. The dip-coating process can be separated into five stages [48, 49]

- 1- Immersion: the substrate is immersed in the solution of the coating material at a constant speed.
- 2- Start-up: the substrate has remained inside the solution for a while and is starting to be pulled up.
- 3- Deposition: the thin layer deposits itself on the substrate while it is pulled up. The withdrawing is carried out at a constant speed to avoid any jitters. The speed determines the thickness of the coating faster withdrawal gives thicker coating material.
- 4- Evaporation: the solvent evaporates from the liquid, forming the thin layer. For volatile solvents, such as alcohols, evaporation starts already during the deposition step.
- 5- Drainage: Excess liquid will drain from the surface.

Prior to deposition the substrates were washed with detergent and then washed with oxidant solution composed of H<sub>2</sub>SO<sub>4</sub> (96% v/v) and H<sub>2</sub>O<sub>2</sub> (29.6% v/v) at 3:1 ratio for 30 minutes. After washing with oxidant solution, all the substrates were rinsed with deionized water. At first, 2 substrates (soda-lime glass) were immersed into the TO sol and TO-TX sol for 10 minutes separately. Furthermore, 2 supporting soda-lime glass plate coated with SO (section 2.3) were immersed into the TO sol and TO-TX sol for 10 minutes. The films were naturally dried in the air and the coating operation was repeated again. The resulting films are denoted as TO, TO-TX, TO- SO and TO-TX-SO. The coated samples were then heat treated at 600 °C for 3 h. furthermore, in order to select the optimum crystallization temperature of TiO<sub>2</sub> film, TO films are calcined at 400 °C and 600 °C for 3h ,separately .

The thickness of the films was increased by repeating the cycles from withdrawing to heating. This procedure carried out six times. According to the Guan method, the average thickness of the films is calculated by means of the weight increase of the films. According to the weight, square and density of the deposited films, the average thickness of each dipping cycle can be calculated [50, 51]. The average thickness of the film was estimated to be ~205 nm.

## 2.5. Characterization of TiO<sub>2</sub> thin films

The crystalline structures of the resulting samples were assessed and characterized by X-ray diffractometer (D4-BRUKER and Cu-K $\alpha$  radiation at 30kv and 20 mA). The chemical structure of the prepared thin film was examined using Fourier Transform Infrared Spectrophotometer (Bio-Rad FTS-165 spectrometer) in the region of 4000 250cm<sup>-1</sup>. Spectra of 300 scans were recorded in room atmosphere under dry air sweeping. Morphological studies were carried out using a scanning electron microscope (SEM) PhilipseXLF30 model and Atomic Force Microscope (AFM, Shimadzu SPM-9500 J2 model. The UV-Vis diffuse reflectance spectra (DRS) of thin films were recorded by UV-Vis spectrophotometer (Shimadzu-2550).

## 2.6. Photocatalytic experiments

The photocatalytic activities of films under UV irradiation were evaluated by the decomposition rate of MCB (C<sub>6</sub>H<sub>6</sub>O) as a model organic compound. All the photocatalytic reactions were carried out in photochemical reactor equipped with 200W quartz lamp which had a maximum power output at 300 nm was used. Also the average intensity of the UV-light is about 3.5mWcm<sup>-2</sup>. 4 samples of thin film (TO, TO-TX, TO- SO and TO-TX-SO) were horizontally placed at the bottom of the testing cell containing

100 mL (100ppm) MCB solution separately. The solution was irradiated with a quartz lamp under ultrasonic stirring. After irradiation, the light absorbance of the MCB solution was measured using a UV-Visible spectrophotometer at 261nm, which is the maximum absorption of MCB.

### 3. Results

#### 3.1 Assessment of crystalline phase

Figure 1(a,b) show the X-ray diffraction pattern of TO film after firing at 400 °C and 600 °C for 3 hours. As can be seen from the figure 1a, TiO<sub>2</sub> film is almost amorphous because no diffraction peaks assignable to its present [42]. The relative peak intensity of the TiO<sub>2</sub> thin film is weaker than those of the TiO<sub>2</sub> powder [52]. This result showed that the growth of the crystallites of the TiO<sub>2</sub> thin films was not grown well as that of TiO<sub>2</sub> powder [53]. As it is shown in fig1b an anatase phase and a quite good crystallization of the films were apparent at 600 °C. We found that the crystallized direction was different for calcination temperatures. In the diffraction pattern of thin film, only wide peak at  $2\theta=25.116^\circ$  corresponding to (101) is observed [54]. It is strongly proposed that such a broad XRD pattern is due to poor crystallization and /or the small size of the TO particles. It should be noted that the crystallite size calculated by Scherrer's formula [55] was 10 nm.

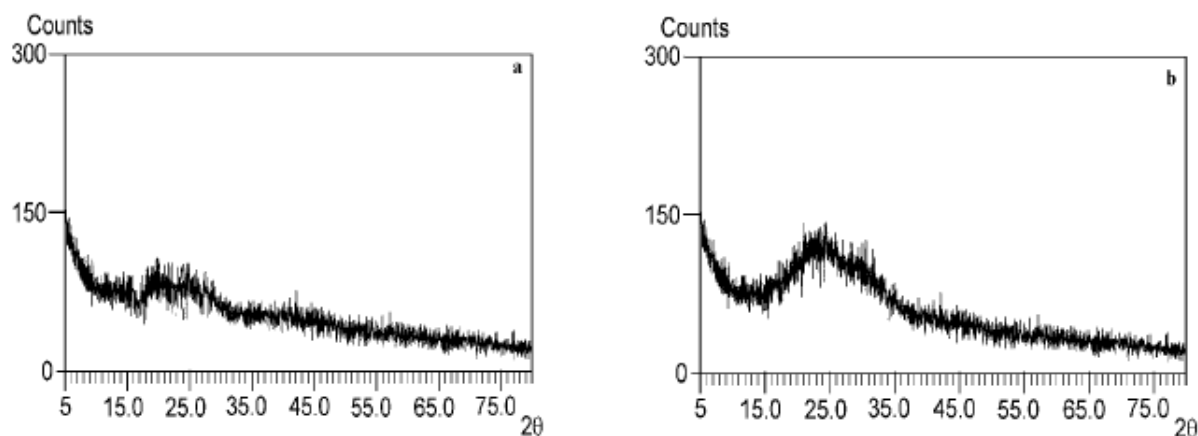
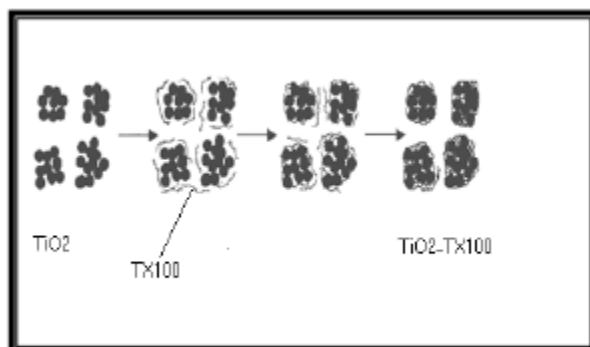


**Figure 1:** X-ray diffraction pattern of TiO<sub>2</sub> thin film on soda lime glass after firing at: (a) 400 °C and (b) 600 °C.

#### 3.2. Mechanism of films formation (TO-TX and TO-SO)

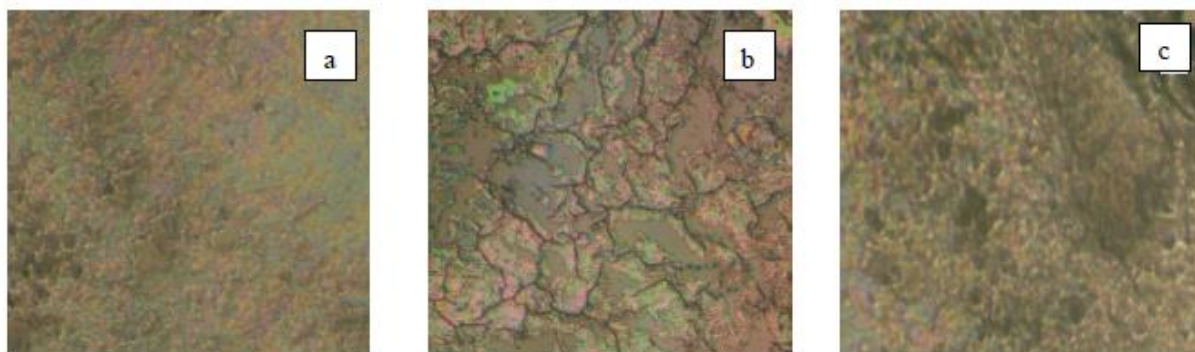
Triton X-100 was used as non-ionic surfactant. TX contains linear alkyl ether chains. At low concentration of TX, probably due to the formation of TO-TX complex, the repulsion between chains is increased leading to slight increase in free volume and further permeation. At higher concentrations of TX, the ether groups in linear alkyl chains of TX can form attraction and binding force between TO chain functional groups. The interaction between alkyl ether and TO chains diminishes the free volume of TO

chains, resulting in permeation diminishment. In the presence of TX, the negative surface charge of the thin layer is decreased, probably due to the formation of a dense and compressed surface, and therefore, Donnan exclusion would be less effective (Fig2).



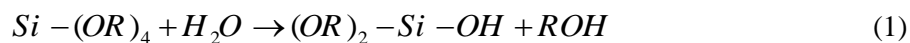
**Figure 2:** The mechanism of TiO<sub>2</sub>-TX100 film formation.

Fig. 3(a-c) shows the light microscopy images of TO–TX film. As can be seen from the figure 3b, the dense and compressed layer is enhanced by adding TX surfactant concentration from 1 to 3 drops. However, with the increase of surfactant concentration to 5 drops, sol viscosity and film thickness increased which lead to destroy Uniformity of the film. As a result, the TX can clearly influences the TO thin layer and changes the morphology of thin layer.

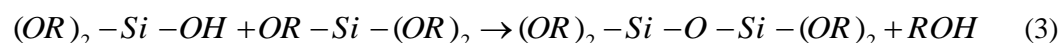
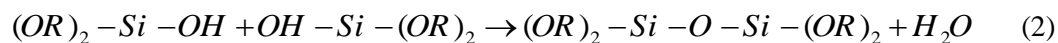


**Figure 3:** The light microscopy images of TiO<sub>2</sub> film: (a) 1 drop of TX100 and (b) 3 drop of TX100 and (c) 5 drop of TX100.

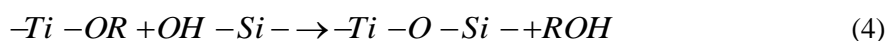
Furthermore, in the presence of water, ethoxy groups of the TEOS precursor are partially hydrolyzed according to the simplified reaction:



Where R is an ethyl group, and thus OR an ethoxy group and ROH ethanol. This reaction describes equilibrium between the hydrolysis of ethoxy groups and the reverse reaction (reesterification). Then, the hydrolyzed groups can react by condensation to form [Si–O–Si] bridging bonds according to the following reactions:



TiO<sub>2</sub> crystallites are diluted in ethanol, ethoxy groups are probably fixed on their surface. Consequently, [- (O-Si) n-] chains diluted in the mixed sol can link on crystallites through a condensation reaction, taking place in the sol or during deposition in liquid phase, according to the simplified reaction (4):



Where [Ti-OR] is an ethoxy group at the TO crystallite surface and [OH-Si] a silanol group at the end of a [- (O-Si) n-] chain. This fixation mechanism is expected to efficiently stabilize silica chains within composite films, whatever the reactivity of the silica sol is. As Fig. 4(a, b) shows FTIR spectra of TO films deposited on Soda lime glass and SO film respectively. Observed peaks at 1070, 950 and 460 cm<sup>-1</sup> indicate asymmetric stretching bands of [Si•••O•••Si] near 1070 cm<sup>-1</sup>, asymmetric stretching bands of [Ti•••O•••Si] around 950 cm<sup>-1</sup> and stretching bands of [Ti•••O] near 460 cm<sup>-1</sup>. The absorption band at about 950 cm<sup>-1</sup> is associated with titanium in four fold coordination with oxygen in the SiO<sub>4</sub> 4-structure. This absorption band confirms the distribution of titanium atoms in [Si•••O•••Si] chains. The broad absorption peak appearing near 3400cm<sup>-1</sup> is related to stretching vibrational aspect of [Ti•••OH] bands, while the absorption peak at 1620 cm<sup>-1</sup> represents [H•••OH] (water) group. It should be mentioned that the intensities of absorption peaks near 1620 and 3400 cm<sup>-1</sup> which appear due to existence of OH group, increased with increasing of silica amount.

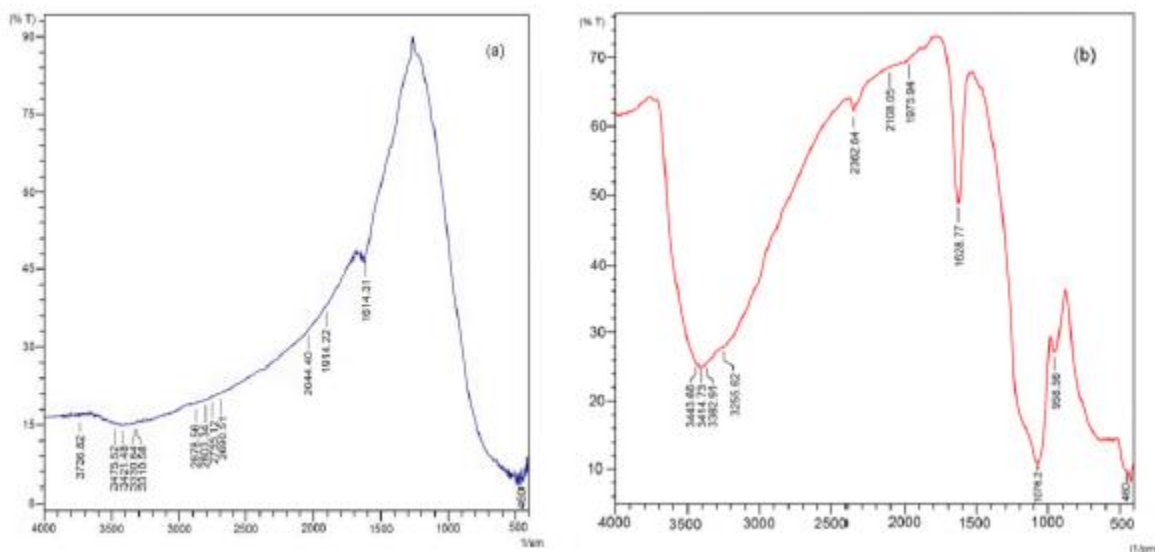
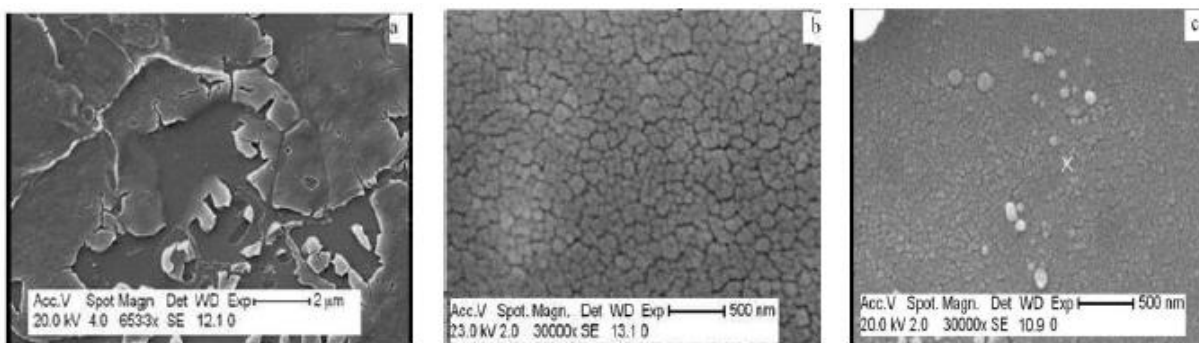


Figure 4: The FT-IR spectra of (a) TiO<sub>2</sub> film and (b) TiO<sub>2</sub>-SiO<sub>2</sub> film.

### 3.3. Surface morphological and topographical analysis

#### 3.3.1. SEM observations

The surface morphology of the TO thin films in the presence and absence of TX and SO are shown in figure (5a-c). It is found that surface structure of the films is greatly dependent on the sols. As it can be seen in Fig. 5a, the film from the TO sol consists of agglomerated titania Particles and ill-defined surface, which may cause the surface to be non-uniform. As a result of agglomeration and non uniform surface, the particle size of this film increased and the surface area decreased which made that unsuitable for photocatalytic degradation of MCB. whereas TO films made with surfactant addition in the sol exhibit a rougher, but still moderately flat texture and well-structured granular nano-surface with clear interstices between the particles /aggregates (Fig. 5b). The TO film deposited on the SO-Coated glass substrate has uniform spherical and narrowly- dispersed particles (Fig 5c). As it can be seen, the accumulation of particles in Fig. 5c indicates packed and dense structure of the TO film. Dense structure with conformal coverage on SO is observed for TO film, whereas in the case of TO films deposited on the bare glass substrate, is not uniform and aggregated TO particles distribute randomly on the surface of soda lime glass. Also, there are many cracks on its surface (Fig. 5a).



**Figure 5:** The SEM patterns of the surface morphology of: (a) TiO<sub>2</sub> film (b) TiO<sub>2</sub>-TX100 film (c) and TiO<sub>2</sub>-SiO<sub>2</sub> film.

A cross-sectional morphology of the thin films by one and six times of coating is shown in Fig. 6(a, b). It can be observed, the number of coating times influences thickness and grain size. Indeed, grain size and thickness increase with increasing the number of coating times [56, 57]. It should be mentioned that film thickness for the one and six times of coating are 181 and 205 nm respectively.

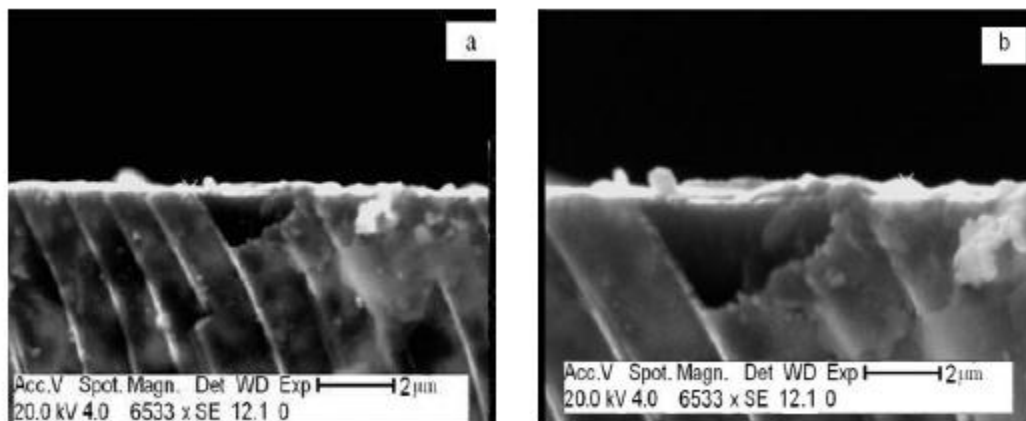


**Figure 6:** The Cross-sectional micrograph for TiO<sub>2</sub> thin film :(a) one time of coating and (b) six times of coating



### 3.3.2. AFM analysis

AFM was used to characterize the surface morphology, particle size, and surface roughness of pure and composite films. As it can be seen from the 2D topographic image in Fig. 7a, the surface of the film deposited from the TO sol is composed of agglomerated titania particles while distribution of the particles on the surface is non-uniform. Furthermore, 3D topographic image also shows the roughness of the surface, which is about 58 nm (Fig.8a).

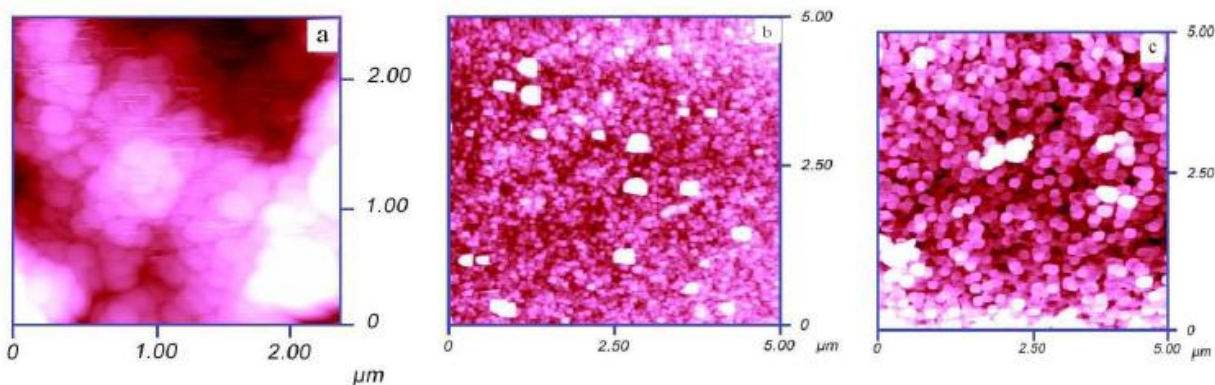


**Figure 7:** The AFM micrograph (2D surface analysis) of the thin films: (a) TiO<sub>2</sub> (b) TiO<sub>2</sub>-TX100 and (c) TiO<sub>2</sub>-SiO<sub>2</sub>.

However, the film from the TX sol is dense and its surface is smooth and uniform, as shown in the 2D topographic image in Fig. 7b. In this case, the roughness profile of the film is 10 nm (Fig.8b). Moreover, in the case of using TX, accumulation of nanoparticles on the thin films is high, while in the absence of TX it is rather low. These results are in good agreement with the above SEM observation in Fig.5. According to figure7c, accumulation of nanoparticles on the surface TO-SO is high and it is clear that the film is uniform and substrate surface is well covered by fine spherical or elliptical grains. While in the film deposited on the bare glass substrate, accumulation of nanoparticles is low (Fig7a). 3D topographic image also shows the roughness of the surface to be about 7.72 nm (Fig8c). The root mean square (rms) surface roughness was determined by using the software which was provided with the microscope.

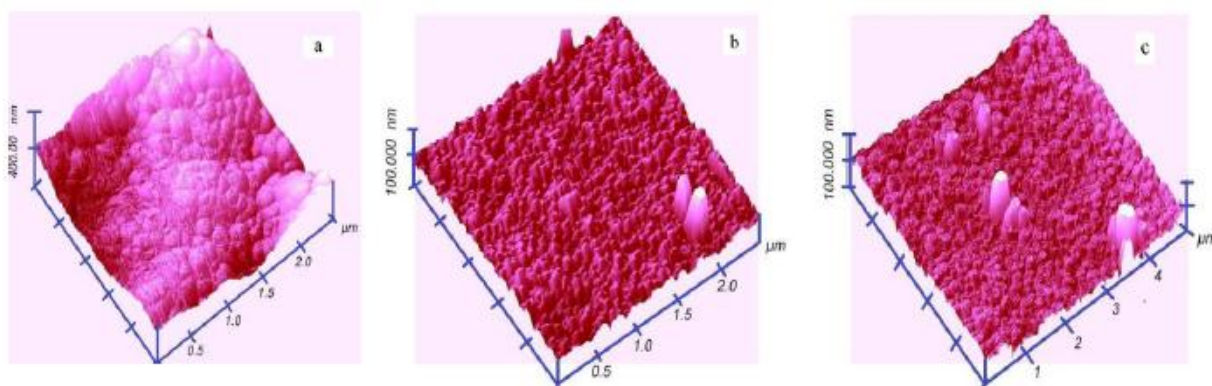


**Figure 8:** The AFM micrograph (3D surface analysis) of thin films: (a) TiO<sub>2</sub> (b) TiO<sub>2</sub>-TX100 and (c) TiO<sub>2</sub>-SiO<sub>2</sub>.

### 3.4. Diffuse reflection spectrum (DRS)

It is necessary to mention that during annealing of films at 600 °C, it is possible that some ions (sodium or calcium) penetrated from glass substrate to the thin films and the effect on film properties. To resolve this problem, before thin film preparation, a thin layer of SO was deposited on glass substrates. This layer was acted as barrier layer. UV-Vis transmittance spectra of TO films deposited on bare and SO-Coated glass substrates are shown in Fig 9.

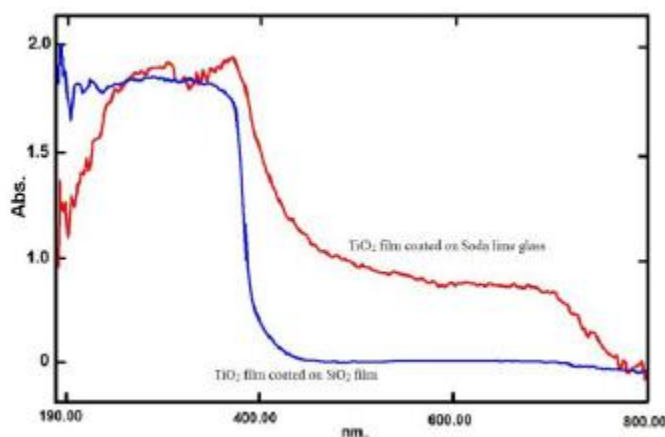


**Figure 9:** The diffuse reflection spectra of TiO<sub>2</sub> films deposited on bare and SiO<sub>2</sub>-Coated glass substrates.

It is clearly seen that TO film deposited on bare glass produced a red-shift of the absorption edge of the film. The shift has been described to differences in the size of the crystallites. The slightly larger anatase grains of films deposited on bare glass substrates may be a consequence of the higher concentration of Na<sup>+</sup> ions diffused from the substrate. Na<sup>+</sup> ions have been found to act as a flux material for crystal growth. It has been also suggested that diffusion of sodium ions from the substrate during thermal treatment could stimulate the recrystallization of the anatase to rutile. Negative solvatochromism corresponds to hypsochromic shift (blue shift) with increasing solvent polarity. Polarity of thin film is related to their chemical structure. Films resulting from interaction of TEOS with TO in film deposited on the SO-Coated glass substrates in comparison to TO films deposited on the bare glass substrate exhibit higher polarity effect. The polarity of films of TO-SO is due to the Ti-O-Si bands. Moreover, addition of TEOS decreases crystal size and crystallinity in TO films particles by inhibiting the growth of particles in the crystalline network. The reduced particle size leads to increased light scattering (an increase in reflectance) and, hence, would result in a decrease in the absorbance. Furthermore, partial hypsochromic shifts indicate the formation of bands between metal (Ti) and binder agent (TEOS) and increasing their polarity.

### 4. Photocatalytic activity

As mentioned in section (2.6), in order to determine was examined while the pH was set on 2, 6 and 9. The obtained results showed that the 1.25 g lit<sup>-1</sup> of TO-TX- SO thin films at pH=2 had the best conditions for degradation of MCB at room temperature (below 40°C) under UV light. Figure (10a-d) shows abatement performances of TO, TO-TX, TO- SO and TO-TX-SO thin films on MCB degradation under UV light. As can be seen from the figures, the maximum absorption peak of MCB at  $\lambda=207$  nm

gradually decreases during the illumination. The illumination time for complete degradation doubles if TO-TX-SO film is compared with TO-TX film, but the difference between TO-TX film and TO-SO film is quite small. After 90 min of illumination, the MCB concentration in case of the TO-TX film is only slightly higher than the TO-SO film. The TO film behaves differently, the degradation is much slower. Compared with the TO-TX-SO, it takes about additional 2.5 h until complete degradation of the dye according to UV-vis spectroscopy. As could be observed, degradation reaction on TO-TX-SO performs in a shorter time (i.e. 90 min) in comparison with TO film (i.e. 240 min), TO-TX film (i.e. 180 min) and TO-SO (i.e. 120 min). Although the absorbance peak area of MCB is decreased for all samples, the largest change arises when TO-TX-SO is used as a photocatalyst. In the case of TO-TX-SO film, it was indicated that when the photocatalytic degradation time reached 30 min, the photocatalytic degradation rates reached more than 60%; as the degradation time increased to 90 min, the photocatalytic degradation rates approached 100%.

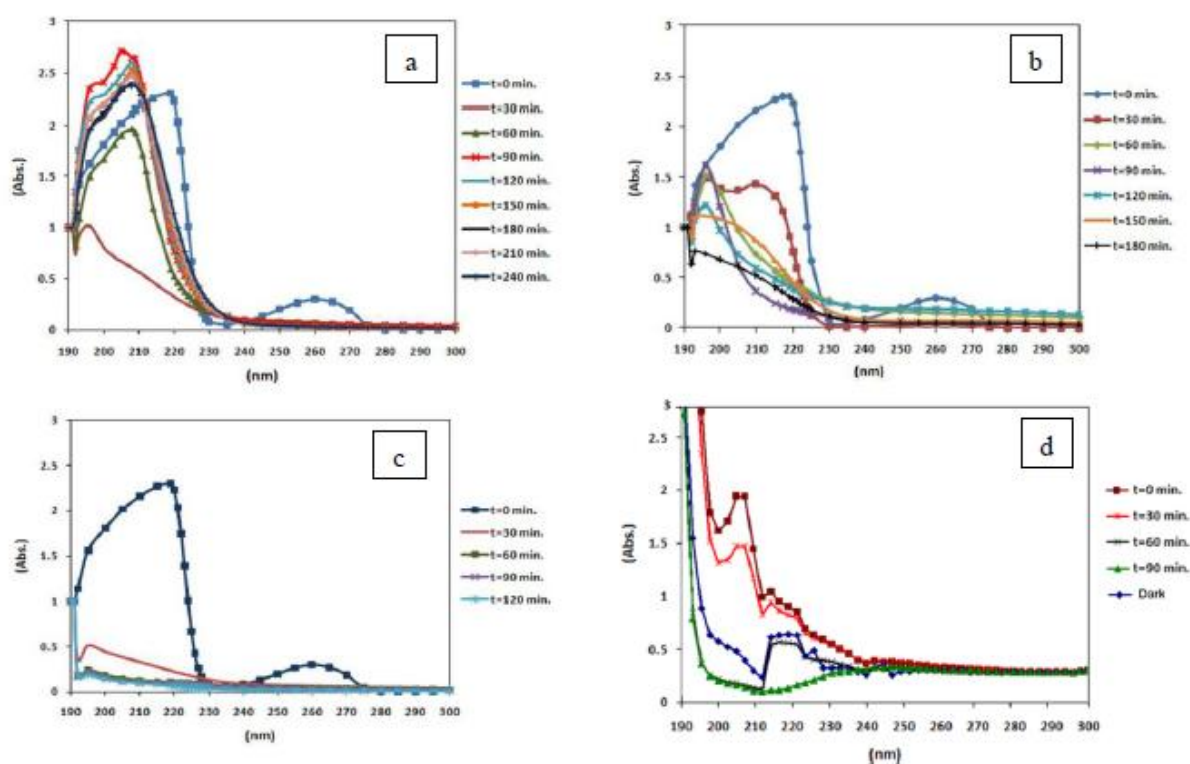


**Figure 10:** Abatement performance of films on MCB degradation under UV light (a)  $\text{TiO}_2$  film (b)  $\text{TiO}_2$ -TX100 film (c)  $\text{TiO}_2$ -  $\text{SiO}_2$  films (d)  $\text{TiO}_2$ -TX100 -  $\text{SiO}_2$ .

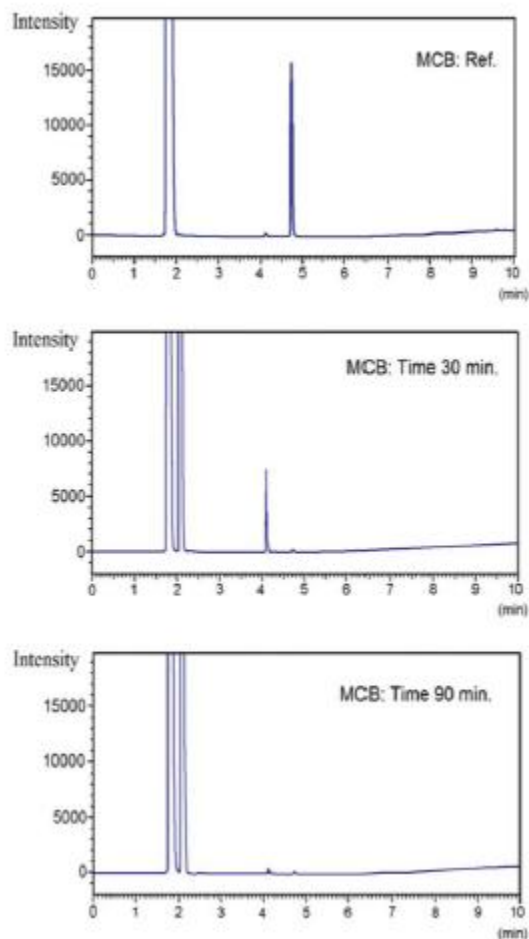
The quantitative analysis of the MCB concentration change after the irradiation of uv light is shown in Table (1).

**Table 1:** Degradation of MCB after irradiation of visible light for 90 min with different photocatalysts.

Photocatalyst	Degradation (%)
$\text{TiO}_2$ =TO	13.2
$\text{TiO}_2$ -TX100=TO-TX	53.72
$\text{TiO}_2$ - $\text{SiO}_2$ =TO-SO	86.02
$\text{TiO}_2$ -TX100- $\text{SiO}_2$ =TO-TX-SO	97.45

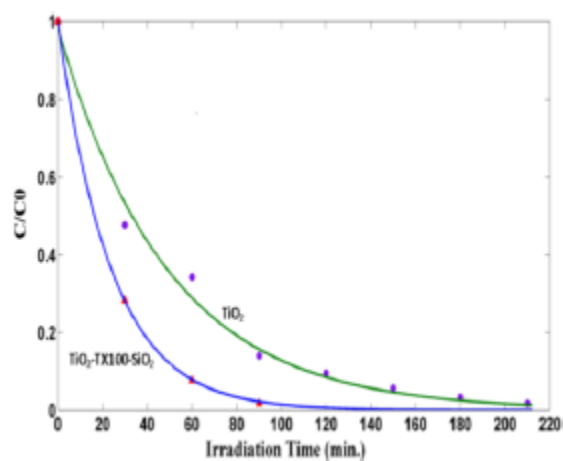
As could be seen, degradation percentage of MCB after the irradiation of uv light for 90 min are 13.2%, 53.72%, 86.02 and 97.45% for TO, TO-TX, TO-SO and TO-TX-SO thin films, respectively. It implies that the photocatalytic property of TiO<sub>2</sub> under the uv light improves when TO is react with SO. In the case of TO-TX- SO film, however, a certain amount of SO in the TO-TX film can lead to an increase of activity in comparison with pure TO or TO-TX films. It should be mentioned that partial changes observed in the absorption intensity of MCB in initial times, are due to the adsorption of MCB on the surface of TO. It is also observed that by using TO-TX- SO photocatalyst, absorption peaks of MCB have been diminished and disappeared after 90 min, whereas in the case of TO film the absorption peaks diminished after 240 minute.

Figure (11) shows the GC analysis of MCB extracted by CH<sub>2</sub>Cl<sub>2</sub> and indicates that by using TO-TX-SO under UV light, there are not any intermediates or byproducts after 90 min of irradiation.



**Figure 11:** The GC analysis of MCB degradation by TiO<sub>2</sub>-TX100 - SiO<sub>2</sub> films under UV light in different times (0, 30 & 90 min).

Concentration changes in photocatalytic degradation of MCB by using TO and TO-TX- SO films are shown in Figures (12) and (13). In these figures variations of  $(C/C_0)$  and  $\ln(C_0/C)$  are presented versus time where  $C_0$  and  $C$  are concentrations of the primal and remaining MCB, respectively. It was found that all curves were linear and accordingly the kinetic data of the MCB photocatalytic photodegradation might fit well to the first-order reaction kinetic model. The rate constants of the apparent first-order reactions rate were estimated from the slopes of the curves. It was demonstrated that the apparent rate constant values of the MCB photocatalytic degradation were  $0.019 \text{ (min}^{-1}\text{)}$  and  $0.045 \text{ (min}^{-1}\text{)}$  for TO and TO-TX- SO photocatalysts, respectively.



**Figure 12:** Photocatalytic degradation kinetics of MCB using  $\text{TiO}_2$  and  $\text{TiO}_2\text{-TX100 - SiO}_2$  (photocatalysts loading,  $1.25 \text{ g lit}^{-1}$ ; initial MBC concentration  $100 \text{ mg lit}^{-1}$ ;  $\text{pH}=2$ ).

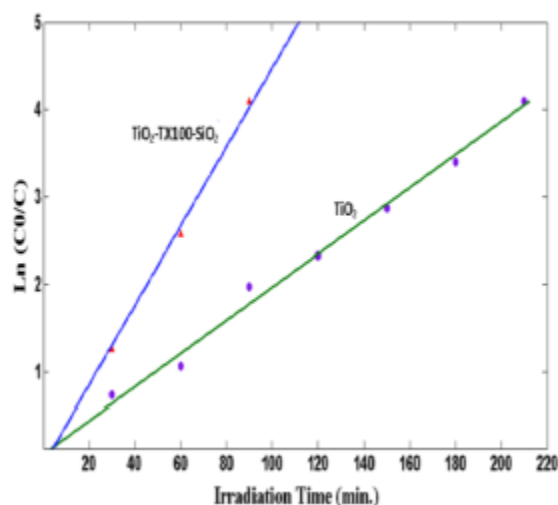


**Figure 13:** The  $\ln(C_0/C)$  vs. time curves of MCB photocatalytic degradation using  $\text{TiO}_2$  and  $\text{TiO}_2\text{-TX100 - SiO}_2$  (photocatalysts loading,  $1.25 \text{ g lit}^{-1}$ ; initial MBC concentration  $100 \text{ mg lit}^{-1}$ ;  $\text{pH}=2$ ).

## 5. Conclusions

It can be concluded that the various additive molecules TX as a surfactant and TEOS as binder agent are the ways to adjust a nano-porous structure of titania films. The film from the TO sol consists of agglomerated titania particles and ill-defined surface, which may cause the surface to be non-uniform, whereas TO films made with surfactant addition in the sol exhibit a rougher, but still moderately flat texture and well-structured granular nanosurface with clear interstices between the particles/aggregates. In fact, the TEOS has an important role to prevent severe cracks on the films during the annealing process at a high temperature. Dense structure with conformal coverage on SO is observed for TO film, whereas in the case of TO films deposited on the bare glass substrate, is not uniform and aggregated TO particles distribute randomly on the surface of soda lime glass. Furthermore, there are many cracks on its surface. Addition of TEOS decreases crystal size and crystallinity in TO films particles by inhibiting the growth of particles in the crystalline network. The reduced particle size leads to increased light scattering (an increase in reflectance) and, hence, would result in a decrease in the absorbance. Furthermore, partial hypsochromic shifts indicate the formation of bands between metal (Ti) and binder agent (TEOS) and increasing their polarity. It can be observed, the number of coating times influences thickness and grain size. Indeed, grain size and thickness increase with increasing the number of coating times. It implies that the photocatalytic property of TO under the uv light improves when TO is react with SO. In the case of TO-TX- SO film, however, a certain amount of SO in the TO-TX film can lead to an increase of activity in comparison with pure TO or TO-TX films.

## Acknowledgements

The authors would like to thank Dr. M.R. Naemijamal for his help in sampling by Atomic Force Microscope.

## References

- [1] D.A Tryk, Recent topics in photoelectrochemistry: achievements and future prospects, *Electrochimica Acta*; **45**(2000) 2363-2376.
- [2] K. Gudea, Adsorption and photocatalytic decomposition of methylene blue on surface modified silica and silica-titania, *Colloids and Surfaces A: Physicochemical and Engineering Aspects*, **325**(2008) 17-20.
- [3] P. Thevenot, J.Cho, D.Wavhal, R.B Timmons, L.P Tang, Surface chemistry influences cancer killing effect of TiO<sub>2</sub> nanoparticles, *Nanomed-Nanotechnol* **4**(2008) 226–236.
- [4] A. Simon-Deckers, B. Gouget, M.Mayne-LHermite, N.Herlin-Boime, C. Reynaud, M. Carriere, In vitro investigation of oxide nanoparticle and carbon nanotube toxicity and intracellular accumulation in A549 human pneumocytes, *Toxicology* **253** (2008) 137–146.
- [5] Y.S Lee, S. Yoon, H.J Yoon, K. Lee, H.K Yoon, J.H Lee, Song.CW, Inhibitor of differentiation 1 (Id1) expression attenuates the degree of TiO<sub>2</sub>-induced cytotoxicity in H1299 non-small cell lung cancer cells, *Toxicol Lett* **189**(2009) 191–199.
- [6] P. Amezaga-Madrid, R. Silveyra-Morales, L. Cordoba-Fierro, G.V.Nevarez- Moorillon, M. Miki-Yoshida, E. Orrantia-Borunda, F.J. Solis, TEM evidence of ultrastructural alteration on *Pseudomonas aeruginosa* by photocatalytic TiO<sub>2</sub> thin films, *J Photoch Photobio* **70** (2003) 45–50.
- [7] M. Hirano, Direct Formation of Anatase (TiO<sub>2</sub>) / Silica (SiO<sub>2</sub>) composite Nanoparticles with high phase stability of 1300 °C from acidic solution by hydrolysis under hydrothermal condition, *Chem. Mater* **16**(2004)3725-3732.
- [8] T.C. Long, N. Saleh, R.D. Tilton, G.V. Lowry, B. Veronesi, Titanium Dioxide (P25) Produces Reactive Oxygen Species in Immortalized Brain Microglia (BV2): Implications for Nanoparticle Neurotoxicity, *Environ. Sci. Technol.* **40** (2006) 4346-4352.

- [9] A. Fujishima, T.N. Rao, D.A. Tryk, Titanium dioxide photocatalysis, *J. Photochem. Photobiol. C* 1 (2000) 1-21.
- [10] N. Arconada, Synthesis and photocatalytic properties of dense and porous TiO<sub>2</sub>-anatase thin films prepared by sol-gel, *Applied Catalysis B: Environmental* **86**(2009)1-7.
- [11] D. Vernardou, One pot direct hydrothermal growth of photoactive TiO<sub>2</sub> films on glass, *Journal of Photochemistry and Photobiology A: Chemistry* **202**(2009) 81-85.
- [12] H. Tian, Photocatalytic degradation of methyl orange with W-doped TiO<sub>2</sub> synthesized by a hydrothermal method. *Materials Chemistry and Physics* **112** (2008) 47-51.
- [13] L. Diamandescu, Structural and photocatalytic properties of iron- and europium-doped TiO<sub>2</sub> nanoparticles obtained under hydrothermal conditions. *Materials Chemistry and Physics* **112**(2008) 146-153.
- [14] V.P. Silva, Silicon rubbers filled with TiO<sub>2</sub>: Characterization and photocatalytic activity, *Materials Chemistry and Physics*, **113**(2009) 395-400.
- [15] R. Dholam, Physically and chemically synthesized TiO<sub>2</sub> composite thin films for hydrogen production by photocatalytic water splitting, *International Journal of Hydrogen Energy* **33**(2008) 6896-6903.
- [16] R.S. Rawat, Nano-phase titanium dioxide thin film deposited by repetitive plasma focus: Ion irradiation and annealing based phase transformation and agglomeration, *Applied Surface Science*, **255**(2008) 2932-2941.
- [17] P. Eiamchai, A spectroscopic ellipsometry study of TiO<sub>2</sub> thin films prepared by ion-assisted electron-beam evaporation, *Current Applied Physics*, **9**(2009) 707-712.
- [18] C. Legnard-Buscema, C. Malibert, S. Bach, Elaboration and characterization of thin films of TiO<sub>2</sub> prepared by sol-gel process, *Thin Solid Films* **418** (2002) 79-84.
- [19] P. Kajitvichyanukul, P. Amornchat, Effects of diethylene glycol on TiO<sub>2</sub> thin film properties prepared by sol-gel process, *Sci. Technol. Adv. Mater.* **6** (2005) 344-347.
- [20] K.S. Liu, H.G. Fu, K.Y. Shi, F.S. Xiao, L.Q. Jing, B.F. Xin, Preparation of Large-Pore Mesoporous Nanocrystalline TiO<sub>2</sub> Thin Films with Tailored Pore Diameters *J. Phys. Chem. B* **109** (2005) 18719-18722.
- [21] L. Zhang, Y.F. Zhu, Y. He, W. Li, H.B. Sun, Preparation and performances of mesoporous TiO<sub>2</sub> film photocatalyst supported on stainless steel, *Appl. Catal. B-Environ.* **40** (2003) 287-292.
- [22] J.K. Liu, T.C. An, G.Y. Li, X.Y. Zeng, N.Z. Bao, G.Y. Sheng, J.M. Fu, Preparation and characterization of highly active mesoporous TiO<sub>2</sub> photocatalysts by hydrothermal synthesis under weak acid conditions, *Micropor. Mesopor. Mater.* **124**(2009) 197-203.
- [23] T.C. An, J.K. Liu, G.Y. Li, S.Q. Zhang, H.J. Zhao, X.Y. Zeng, G.Y. Sheng, J.M. Fu, Structural and photocatalytic degradation characteristics of hydrothermally treated mesoporous TiO<sub>2</sub> *Appl. Catal. A-Gen.* **350** (2008) 237-243.
- [24] U. Cernigoj, U. L. Stangar, P. Trebxe, U. O. Kraxovec, S. Gross, Photocatalytically active TiO<sub>2</sub> thin films produced by surfactant-assisted sol-gel processing, *Thin Solid Films* **495** (2006) 327 - 332.
- [25] M. Cozzolino, Grafting of titanium alkoxides on high- surface SiO<sub>2</sub> support: An advanced technique for the preparation of nanostructured TiO<sub>2</sub>/SiO<sub>2</sub> catalysts. *Applied Catalysis A: General* **325**(2007) 256-262.
- [26] M. Harada, Preparation and characterizations of Fe- or Ni-substituted titania nanosheets as photocatalysts, *J. Photochem. Photobiol. A: Chem* **148**(2002) 273-276.
- [27] Z.M Shi, Study of crystallization behavior of Ce<sup>4+</sup> modified titania gels, *Scripta Mater* **50**(2004) 885-889.
- [28] S. Yoshinaka, Hydrodesulfurization of dibenzothiophenes over molybdenum catalyst supported on TiO<sub>2</sub>-Al<sub>2</sub>O<sub>3</sub>, *Catal. Today* **45** (1998) 293-298.
- [29] K.Y. Jung, Photoactivity of SiO<sub>2</sub>/TiO<sub>2</sub> and ZrO<sub>2</sub>/TiO<sub>2</sub> mixed oxides prepared by sol-gel method, *Mater. Lett* **58**(2004) 2879-2900.
- [30] G. Xu, Effect of silica on the microstructure and photocatalytic properties of titania, *Ceramic International* **35**(2009) 1-5.
- [31] K.V. Baiju, Enhanced photoactivity and anatase thermal stability of silica-alumina mixed oxide additives on sol-gel nanocrystalline titania, *Materials Letters* **61**(2007) 1751-1755.
- [32] A.L. Castro, Synthesis of anatase TiO<sub>2</sub> nanoparticles with high temperature stability and photocatalytic activity, *Solid State Sciences* **10**(2008) 602-606.
- [33] P. Periyat, High temperature stable mesoporous anatase TiO<sub>2</sub> photocatalyst achieved by silica addition. *Applied Catalysis A: General* **349**(2008) 13-19.
- [34] S. Zhu, Preparation and Performance of Al<sub>2</sub>TiO<sub>5</sub>-TiO<sub>2</sub>-SiO<sub>2</sub> Honeycomb Ceramics by Doping Rare Earth. *Journal of Rare Earths* **25**(2007) 457-461.
- [35] J. Guo, Activity and stability of iron-containing pillared clay catalysts for wet air oxidation of phenol. *Applied Catalysis A: General*, **299**(2006) 175-184.

- [36] S.J Yoon, Synthesis of TiO<sub>2</sub>-entrapped EFAL-removed Y-zeolites. Novel photocatalyst for decomposition of 2-methylisoborneol, *Catalysis Communications* **8**(2007) 1851-1856.
- [37] S. Anandan. Photocatalytic effects of titania supported nanoporous MCM-41 on degradation of methyl orange in the presence of electron acceptors, *Dyes and Pigments* **76**(2008) 535-541.
- [38] Y.A Kim, Preparation of high porous Pt-V<sub>2</sub>O<sub>5</sub>-WO<sub>3</sub>/TiO<sub>2</sub>/SiC filter for simultaneous removal of NO and particulates, *Powder Technology* **180**(2008) 79-85.
- [39] S .Chen, Theoretical simulation of the interaction between neighboring oxygen ions for cation and anion-doped c-ZrO<sub>2</sub>. *Materials Chemistry and Physics* **103**(2007) 28-34.4
- [40] Y. Arai, Photocatalysis of SiO<sub>2</sub>-loaded TiO<sub>2</sub>, *Journal of Molecular Catalysis A: Chemical* **243**(2006) 85-88.
- [41] H. Samari Jahromi , H. Taghdisian S. Afshar ,S. Tasharofi, Effects of pH and polyethylene glycol on surface morphology of TiO<sub>2</sub> thin film, *Surface & Coatings Technology* **203** (2009) 1991-1996.
- [42] Y. Djaoued, S. Badilescu, P. Vashrit, D. Bersani, P.P. Lottici, J. Robichaud, study of anatase to rutile phase transition in nanocrystalline titania films, *J. Sol-Gel Sci. Technol.* **24** (2002) 255-264.
- [43] B. Guo, Z. Liu, L. Hong, H. Jiang, Sol gel derived photocatalytic porous TiO<sub>2</sub> thin films ,*Surf. Coat. Technol.* **198** (2005) 24-29.
- [44] S.J. Bu, G. Lin, X.X. Liu, L.R. Yang, Z.J. Cheng, Synthesis of TiO<sub>2</sub> porous thin films by polyethylene glycol templating and chemistry of the process *J. Europ. Ceram. Soc.* **25** (2005) 673-679.
- [45] J. Yu, X. Zhao, Q. Zhao, Effect of surface structure on photocatalytic activity of TiO<sub>2</sub> thin films prepared by sol-gel method, *Thin Solid Film* **379** (2000) 7-14.
- [46] Y. Chen, S. Lunsford, D.D. Dionysiou, Photocatalytic activity and electrochemical response of titania film with macro/mesoporous texture *Thin Solid Films* **516** (2008) 7930-7936.
- [47] Y. Chen, D.D. Dionysiou, Effect of calcination temperature on the photocatalytic activity and adhesion of TiO<sub>2</sub> films prepared by the P-25 powder-modified sol-gel method, *J. Mol. Catal. A: Chem.* **244** (2006) 73-82.
- [48] L.E. Scriven, Physics and applications of dip coating and spin coating, *Better ceramics through chemistry III.* (1988) 717-729.
- [49] M.N. Rahaman, *Ceramic Processing*, Boca Raton: CRC Press (2007)242-244.
- [50] K. Guan, Relationship between photocatalytic activity, hydrophilicity and self cleaning effect of TiO<sub>2</sub>/SiO<sub>2</sub> films ,*Surf. Coat. Technol.* **191**(2005) 155.
- [51] A. Eshaghi, A.Eshaghi, Self-cleaning Properties of TiO<sub>2</sub>-SiO<sub>2</sub>-In<sub>2</sub>O<sub>3</sub> Nanocomposite Thin Film, *Bull. Korean Chem. Soc* **32**(2011) 3991-3995.
- [52] H. S. Jahromi, H. Taghdisian, S. Tasharofi, Synthesis of TiO<sub>2</sub> nanopellet by TiCl<sub>4</sub> as a precursor for degradation of RhodamineB, *Materials Chemistry and Physics* **122** (2010) 205-210.
- [53] D. Tiwari, S. M. Lee, Y. H. Kim, Alka and K. M. Choi, Synthesis of TiO<sub>2</sub> using Sol-Gel method and Comparison of Photo catalytic Characteristics, *Proceedings of the 3rd International CEMEPE & SECOTOX Conference Skiathos, June 19-24* (2011).
- [54] J.C. Yu, X.C. Wang, X.Z. Fu, Pore-Wall Chemistry and Photocatalytic Activity of Mesoporous Titania Molecular Sieve Films, *Chem. Mater.* **16** (2004) 1523-1530.
- [55] J.G. Yu, H.G. Yu, B. Cheng, X.J. Zhao, J.C. Yu, W.K. Ho, The Effect of Calcination Temperature on the Surface Microstructure and Photocatalytic Activity of TiO<sub>2</sub> Thin Films Prepared by Liquid Phase Deposition, *J. Phys. Chem. B* **107** (2003) 13871-13879.
- [56] S. Çorekçia, K. Kızılkayab, T. Asarb, M.K. Öztürkb, M. Çakmakb and S. Özçelıkb, Effects of Thermal Annealing and Film Thickness on the Structural and Morphological Properties of Titanium Dioxide Films, *Acta Physica PolonicaA.* **121**(2012)247-248.
- [57] M. Viana, D. S. Mohallem, L. T. Nascimento, and D. S. Mohallem, Nanocrystalline Titanium Oxide thin Films Prepared by Sol-Gel Process, *Brazilian Journal of Physics* **36**(2006)1081-1083.